Papers in Physics, vol. 2, art. 020008 (2010)

www.papersinphysics.org

Received: 20 October 2010, Accepted: 1 December 2010
Edited by: A. Vindigni
Reviewed by: A. A. Fedorenko, CNRS-Lab. de Physique, ENS de Lyon, France.

DOI: 10.4279/PIP.020008

ISSN 1852-4249

# Anisotropic finite-size scaling of an elastic string at the depinning threshold in a random-periodic medium

S. Bustingorry,[1]* A. B. Kolton[1]†

We numerically study the geometry of a driven elastic string at its sample-dependent depinning threshold in random-periodic media. We find that the anisotropic finite-size scaling of the average square width $\overline{w^2}$ and of its associated probability distribution are both controlled by the ratio $k = M/L^{\zeta_{\rm dep}}$, where $\zeta_{\rm dep}$ is the random-manifold depinning roughness exponent, $L$ is the longitudinal size of the string and $M$ the transverse periodicity of the random medium. The rescaled average square width $\overline{w^2}/L^{2\zeta_{\rm dep}}$ displays a non-trivial single minimum for a finite value of $k$. We show that the initial decrease for small $k$ reflects the crossover at $k \sim 1$ from the random-periodic to the random-manifold roughness. The increase for very large $k$ implies that the increasingly rare critical configurations, accompanying the crossover to Gumbel critical-force statistics, display anomalous roughness properties: a transverse-periodicity scaling in spite that $\overline{w^2} \ll M$, and subleading corrections to the standard random-manifold longitudinal-size scaling. Our results are relevant to understanding the dimensional crossover from interface to particle depinning.

## I. Introduction

The study of the static and dynamic properties of $d$-dimensional elastic interfaces in $d+1$-dimensional random media is of interest in a wide range of physical systems. Some concrete experimental examples are magnetic [1–4] or ferroelectric [5,6] domain walls, contact lines of liquids [7], fluid invasion in porous media [8, 9], and fractures [10, 11]. In all these systems, the basic physics is controlled by the competition between quenched disorder (induced by the presence of impurities in the host materials) which promotes the wandering of the elastic object, against the elastic forces which tend to make the elastic object flat. One of the most dramatic and worth understanding manifestations of this competition is the response of these systems to an external drive.

The mean square width or roughness of the interface is one of the most basic quantities in the study of pinned interfaces. In the absence of an external drive, the ground state of the system is disordered but well characterized by a self-affine rough geometry with a diverging typical width $w \sim L^{\zeta_{\rm eq}}$, where $L$ is the linear size of the elastic object and $\zeta_{\rm eq}$ is the equilibrium roughness exponent. When the external force is increased from zero, the ground state becomes unstable and the interface is locked in metastable states. To overcome the barriers separating them and reach a finite steady-state velocity $v$ it is necessary to exceed a finite critical force, above which barriers disappear and no metastable states exist. For directed $d$-dimensional elastic interfaces with convex elastic energies in a $D = d+1$ dimensional space with disorder, the critical point

*E-mail: sbusting@cab.cnea.gov.ar
†E-mail: koltona@cab.cnea.gov.ar

[1] CONICET, Centro Atómico Bariloche, 8400 San Carlos de Bariloche, Río Negro, Argentina.

is unique, characterized by the critical force $F = F_c$ and its associated critical configuration [12]. This critical configuration is also rough and self-affine such that $w \sim L^{\zeta_{\rm dep}}$ with $\zeta_{\rm dep}$ the depinning roughness exponent. When approaching the threshold from above, the steady-state average velocity vanishes like $v \sim (F - F_c)^{\beta}$ and the correlation length characterizing the cooperative avalanche-like motion diverges as $\xi \sim (F - F_c)^{-\nu}$ for $F > F_c$, where $\beta$ is the velocity exponent and $\nu$ is the depinning correlation length exponent [13–16]. At finite temperature and for $F \ll F_c$, the system presents an ultra-slow steady-state creep motion with universal features [17, 18] directly correlated with its multi-affine geometry [19,20]. At very small temperatures the absence of a divergent correlation length below $F_c$ shows that depinning must be regarded as a non-standard phase transition [20, 21] while exactly at $F = F_c$, the transition is smeared-out with the velocity vanishing as $v \sim T^{\psi}$, with $\psi$, the so-called thermal rounding exponent [22–27].

During the last years, numerical simulations have played an important role to understand the physics behind the depinning transition thanks to the development of powerful exact algorithms. In particular, the development of an exact algorithm able to target efficiently the critical configuration and critical force for a given sample [28, 29] has allowed to study, precisely, the self-affine rough geometry at depinning [7, 28–31], the sample-to-sample critical force distribution [32], the critical exponents of the depinning transition [26, 27, 33], the renormalized disorder correlator [34], and the avalanche-size distribution in quasistatic motion [35]. Moreover, the same algorithm has allowed to study, precisely, the transient universal dynamics at depinning [36, 37], and an extension of it has allowed to study low-temperature creep dynamics [20, 21].

In practice, the algorithm for targeting the critical configuration [28, 29] has been numerically applied to directed interfaces of linear size $L$ displacing in a disordered potential of transverse dimension $M$, applying periodic boundary conditions in both directions in order to avoid border effects. This is thus equivalent to an elastic string displacing in a disordered cylinder. The aspect ratio between longitudinal $L$ and transverse $M$ periodicities must be carefully chosen, in order to have the desired thermodynamic limit corresponding to a given experimental realization. In Ref. [32] it was indeed shown that the critical force distribution $P(F_c)$ displays three regimes associated with $M$: (i) At very small $M$ compared with the typical width $L^{\zeta_{\rm dep}}$ of the interface, the interface wraps the computational box several times in the transverse direction, as shown schematically in Fig. 1(b), and therefore the periodicity of the random medium is relevant and $P(F_c)$ is Gaussian; (ii) At very large $M$ compared with $L^{\zeta_{\rm dep}}$, as shown schematically in Fig. 1(c), periodicity effects are absent but then the critical force, being the maximum among many independent sub-critical forces, obeys extreme value statistics and $P(F_c)$ becomes a Gumbel distribution; (iii) In the intermediate regime, where $M \approx L^{\zeta_{\rm dep}}$ and periodicity effects are still irrelevant, as shown schematically in Fig. 1(a), the distribution function is in between the Gaussian and the Gumbel distribution. It has been argued that only the last case, where $M \approx L^{\zeta_{\rm dep}}$, corresponds to the random-manifold depinning universality class (periodicity effects absent) with a finite critical force in the thermodynamic limit $L, M \to \infty$. This criterion does not give, however, the optimal value of the proportionality factor between $M$ and $L^{\zeta_{\rm dep}}$, and must be modified at finite velocity since the crossover to the random-periodic universality class at large length-scales depends also on the velocity [38]. To avoid this problem, it has been therefore proposed to define the critical scaling in the fixed center of mass ensemble [39]. The crossover from the random-manifold to the random-periodic universality class is, however, physically interesting, as it can occur in periodic elastic systems such as elastic chains. Remarkably, although the mapping from a periodic elastic system (with given lattice parameter) in a random potential to a non-periodic elastic system (such as an interface) in a random potential with periodic boundary conditions is not exact, it was recently shown that the lattice parameter does play the role of $M$ for elastic interfaces with regard to the geometrical or roughness properties [38]. Since the periodicity can often be experimentally tuned in such periodic systems it is thus worth studying in detail the geometry of critical interfaces of size $L$ as a function of $M$ with periodic boundary conditions, and thus complement the study of the critical force in such systems [32].

In this paper, we study in detail, using numerical simulations, the geometrical properties of the one-

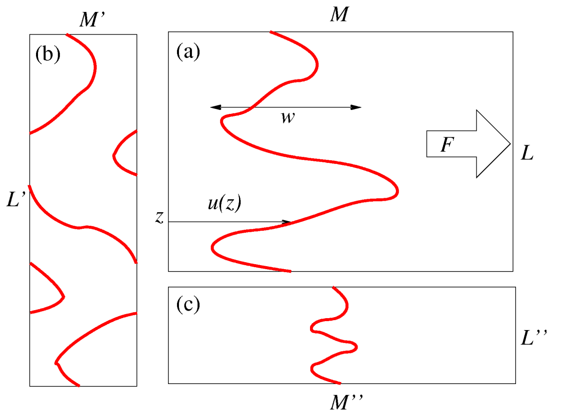


Figure 1: (a) Elastic string driven by a force $F$ in a random-periodic medium with periodic boundary conditions. It is described by a displacement field $u(z)$ and has a mean width $w$. The anisotropic finite-size scaling of width fluctuations are controlled by the aspect-ratio parameter $k = M/L^{\zeta_{\rm dep}}$, with $\zeta_{\rm dep}$ the random-manifold roughness exponent at depinning. In the case $k \ll 1$ (b) periodicity effects are important, while when $k \gg 1$ (c) they are not important but the roughness scaling of the critical configuration is anomalous.

dimensional interface or elastic string critical configuration in a random-periodic pinning potential as a function of the aspect ratio parameter $k$, conveniently defined as $k = M/L^{\zeta_{\rm dep}}$. We show that $k$ is indeed the only parameter controlling the finite-size scaling (i.e. the dependence of observables with the dimensions $L$ and $M$) of the average square width and its sample-to-sample probability distribution. The scaled average square width $\overline{w^2}L^{-2\zeta_{\rm dep}}$ is described by a universal function of $k$ displaying a non-trivial single minimum at a finite value of $k$. We show that while for small $k$ this reflects the crossover at $k \sim 1$ from the random-periodic to the random-manifold depinning universality class, for large $k$ it implies that in the regime where the depinning threshold is controlled by extreme value (Gumbel) statistics, critical configurations also become rougher, and display an anomalous roughness scaling.

# II. Method

The model we consider here is an elastic string in (1+1) dimensions described by a single valued function $u(z,t)$, which gives the transverse displacement $u$ as a function of the longitudinal direction $z$ and the time $t$ [see Fig. 1(a)]. The zero-temperature dynamics of the model is given by

$$\gamma\,\partial_t u(z,t) = c\,\partial_z^2 u(z,t) + F_p(u,z) + F, \qquad (1)$$

where $\gamma$ is the friction coefficient and $c$ the elastic constant. The first term in the right hand side derives from an harmonic elastic energy. The effects of a random-bond type disorder is given by the pinning force $F_p(u,z) = -\partial_u U(u,z)$. The disorder potential $U(u,z)$ has zero average and sample-to-sample fluctuations given by

$$\overline{[U(u,z) - U(u',z')]^2} = \delta(z-z')\,R^2(u-u'), \qquad (2)$$

where the overline indicates average over disorder realizations and $R(u)$ stands for a correlator of finite range $r_f$ [18]. Finally, $F$ represents the uniform external drive acting on the string. Physically, this model can phenomenologically describe, for instance, a magnetic domain wall in a thin film ferromagnetic material with weak and randomly located imperfections [1], being $F$ proportional to an applied external magnetic field pushing the wall in the energetically favorable direction.

In order to numerically solve Eq. (1), the system is discretized in the $z$-direction in $L$ segments of size $\delta z = 1$, i.e. $z \to j = 0, ..., L-1$, while keeping $u_j(t)$ as a continuous variable. To model the continuous random potential, a cubic spline is used, which passes through $M$ regularly spaced uncorrelated Gaussian number points [30]. For the numerical simulations performed here we have used, without loss of generality, $\gamma = 1$, $c = 1$ and $r_f = 1$ and a disorder intensity $R(0) = 1$. In both spatial dimensions we have used periodic boundary conditions, thus defining a $L \times M$ system.

The critical configuration $u_c(z)$ and force $F_c$ are defined from the pinned (zero-velocity) configuration with the largest driving force $F$ in the long time limit dynamics. They are thus the real solutions of

$$c\,\partial_z^2 u(z) + F_p(u,z) + F = 0, \qquad (3)$$

such that for $F > F_c$ there are no further real solutions (pinned configurations). Middleton theorems [12] assure that for Eqs. (3) the solution exists and it is unique for both $u_c(z)$ and $F_c$, and that above $F_c$ the string trajectory in an $L$ dimensional phase-space is trapped into a periodic attractor (for a system with periodic boundary conditions as the one we consider). In other words, the critical configuration is the marginal fixed point solution or critical state of the dynamics, being $F_c$ the critical point control parameter of a Hopf bifurcation. Solving the $L$-dimensional system of Eqs. (3) for large $L$ directly is a formidable task, due to the non-linearity of the pinning force $F_p$. On the other hand, solving the long-time dynamics at different driving forces $F$ to localize $F_c$ and $u_c$ is very inefficient due to the critical slowing down. Fortunately, Middleton theorems, and in particular the "non-passing rule", can be used again to devise a precise and very efficient algorithm which allows to obtain the critical force $F_c$ and the critical configuration $u_j^c$ for each independent disorder realization iteratively without solving the actual dynamics nor directly inverting the system of Eqs. (3) [30]. Once the critical force and the critical configuration are determined with this algorithm, we can compute the different observables. In particular, the square width or roughness of the string at the critical point for a given disorder realization is defined as

$$w^2 = \frac{1}{L}\sum_{j=0}^{L-1}\left[u_j^c - \frac{1}{L}\sum_{k=0}^{L-1} u_k^c\right]^2 . \tag{4}$$

Computing $w^2$ for different disorder realizations allows us to compute its disorder average $\overline{w^2}$ and the sample-to-sample probability distribution $P(w^2)$. In addition, the average structure factor associated to the critical configuration is

$$S_q = \frac{1}{L}\overline{\left|\sum_{j=0}^{L-1} u_j^c\, e^{-iqj}\right|^2} , \tag{5}$$

where $q = 2\pi n/L$, with $n = 1, ..., L-1$. One can show, using a simple dimensional analysis, that given a roughness exponent $\zeta$, such that $\overline{w^2} \sim L^{2\zeta}$, the structure factor behaves as $S(q) \sim q^{-(1+2\zeta)}$ for small $q$, thus yielding an estimate to $\zeta$ without changing $L$. To compute averages over disorder and sample-to-sample fluctuations, we consider between $10^3$ and $10^4$ independent disorder realizations depending on the size of the system.

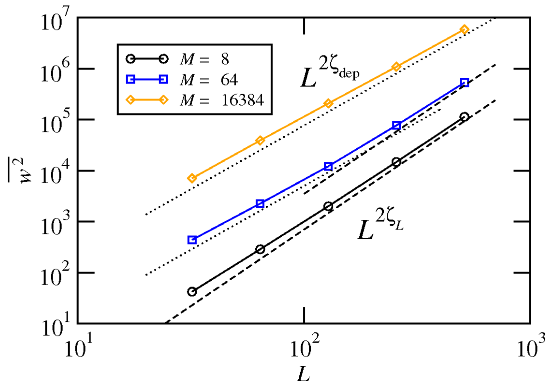


Figure 2: The scaling of $\overline{w^2}$ for the critical configuration at different $M$ values as indicated. The curves for $M = 64$ and 16384 are shifted upwards for clarity. The dashed and dotted lines are guides to the eye showing the expected slopes corresponding to the different roughness exponents.

## III. Results

### i. Roughness at the critical point

Figure 2 shows the scaling of the square width of the critical configuration $\overline{w^2}$ with the longitudinal size of the system $L$ for $L = 32, 64, 128, 256, 512$ and different values of $M$. When $M$ is small, $M = 8$, for all the $L$ values shown we observe $\overline{w^2} \sim L^{2\zeta_{\rm L}}$ with $\zeta_{\rm L} = 1.5$, corresponding to the Larkin exponent in $(1+1)$ dimensions. This value is different from the value $\zeta_{\rm dep} = 1.25$ [33, 40] expected for the random-manifold universality class, and is thus indicating that the periodicity effects are important for this joint values of $M$ and $L$. This situation is schematically represented in Fig. 1(b). This result is a numerical confirmation of the two-loop functional renormalization group result of Ref. [16] which shows that the $\zeta = 0$ fixed point, leading to a universal logarithmic growth of displacements at equilibrium is unstable. The fluctuations are governed, instead, by a coarse-grained generated random-force as in the Larkin model, yielding a roughness exponent $\zeta_{\rm L} = (4-d)/2$ in $d$ dimensions [16], which agrees with our result for $d = 1$. We can thus say

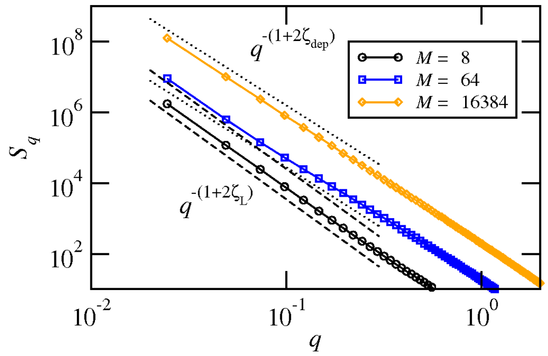


Figure 3: Structure factor of the critical configuration for $L = 256$ and different $M$ values, as indicated. The curves for $M = 64$ and 16384 are shifted upwards for clarity. The dashed and dotted lines are guides to the eye showing the expected slopes corresponding to the different roughness exponents.

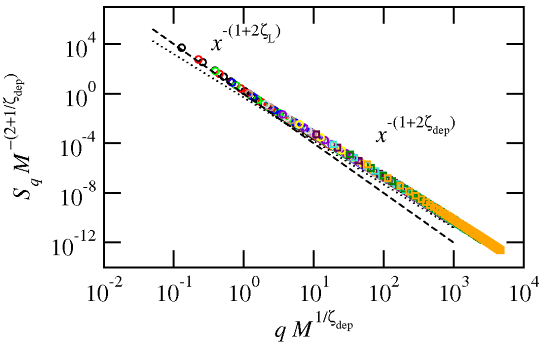


Figure 4: Scaling of the structure factor of the critical configuration for $L = 256$ and different values of the transverse size $M = 2^p$ with $p = 3, 4, ..., 14$ $M$. Although the values of the two exponents are very close, the change in the slope of the scaling function against the scaling variable $x = q\,M^{1/\zeta_{\rm dep}}$ is clearly observed.

that for small enough $M$ (compared to $L$) the system belongs to the same random-periodic depinning universality class as charge density wave systems [14,41], which strictly correspond to $M = 1$.

When $M$ is large, on the other hand, $M = 16384$ in Fig. 2, for all the $L$ values considered the exponent is consistent with $\zeta_{\rm dep}$, of the random-manifold universality class. This situation is schematically represented in Fig. 1(c), and we will show later that, for this elongated samples, the effects of extreme value statistics are already visible.

For intermediate values of $M$, such as $M = 64$ in Fig. 2, we can observe the crossover in the scale-dependent roughness exponent $\zeta(L) \sim \frac{1}{2}\frac{d\log w^2}{d\log L}$ changing from $\zeta_{\rm dep}$ to $\zeta_{\rm L}$ as $L$ increases, as indicated by the dashed and dotted lines. This crossover, from the random-manifold to the random-periodic depinning geometry, occurs at a characteristic distance $l^* \sim M^{1/\zeta_{\rm dep}}$, when the width in the random-manifold regime reaches the transverse dimension or periodicity $M$. At finite velocity, this crossover length remains constant up to a non-trivial characteristic velocity and then decreases with increasing velocity [38].

The above mentioned geometrical crossover can be studied in more details through the analysis of the structure factor $S(q)$, for a line of fixed size $L$. In Fig. 3 we show $S(q)$ for $L = 256$ and $M = 8, 64, 16384$. For the intermediate value $M = 64$ a crossover between the two regimes is visible, and can be described by

$$S_q \sim \left\{ \begin{array}{ll} q^{-(1+2\zeta_{\rm L})} & q \ll q^*, \\ q^{-(1+2\zeta_{\rm dep})} & q \gg q^*. \end{array} \right. \qquad (6)$$

with $q^*$ expected to scale as $q^* \sim l^{*-1} \sim M^{-1/\zeta_{\rm dep}}$. Therefore, the structure factor should scale as $S_q M^{-(2+1/\zeta_{\rm dep})} = H(x)$, where the scaled variable is $x = q\,M^{1/\zeta_{\rm dep}} \sim q/q^*$ and the scaling function behaves as

$$H(x) \sim \left\{ \begin{array}{ll} x^{-(1+2\zeta_{\rm L})} & x \ll 1, \\ x^{-(1+2\zeta_{\rm dep})} & x \gg 1. \end{array} \right. \qquad (7)$$

The collapse of Fig. 4 for $L = 256$ and different values of $M = 2^p$ with $p = 3, 4, ..., 14$ shows that this scaling form is a very good approximation. However, as we show below, small corrections can be expected fully in the random-manifold regime in the large $ML^{-\zeta_{\rm dep}}$ limit of very elongated samples.

In Fig. 5(a), we show $\overline{w^2}$ as a function of the transverse periodicity $M$ for different values of the longitudinal periodicity $L$. Remarkably, $\overline{w^2}$ is a non-monotonic function of $M$. For small $M$ it decreases towards an $L$ dependent minimum $m^*$, and then increases with increasing $M$, in the regime where the extreme value statistics starts to affect the distribution of the critical force [32]. Since

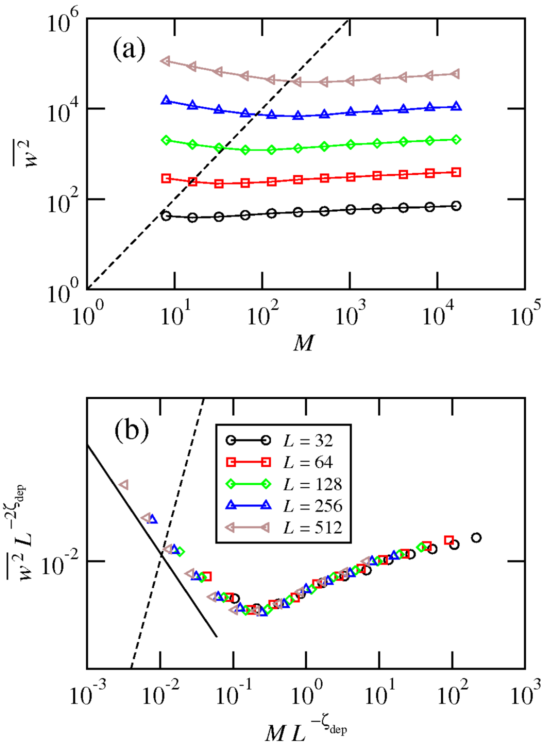


Figure 5: (a) Squared width of the critical configuration as a function of $M$ for different system sizes $L$ as indicated. (b) Scaling of the width in (a), showing that the relevant control parameter is $M/L^{\zeta_{\rm dep}}$. The dashed line in (a) and (b) corresponds to $\overline{w^2} = M^2$, which is always to the left of the minimum of $\overline{w^2}$ occurring at $k^* = m^* L^{-\zeta_{\rm dep}}$. The solid line indicates $k^{2(1-\zeta_{\rm L}/\zeta_{\rm dep})}$ which is the behavior expected purely from the random-periodic to random-manifold crossover at the characteristic distance $l^* \sim M^{1/\zeta_{\rm dep}}$.

the only typical transverse scale in Fig. 5(a) is set by the minimum $m^*$, we can expect $\overline{w^2} \sim m^{*2} G(M/m^*)$ with $G(x)$ some universal function. On the other hand, since the only relevant characteristic length-scale of the problem is set by the crossover between the random-periodic regime and the random-manifold regime, we can simply write $m^* \sim L^{\zeta_{\rm dep}}$ and therefore

$$\overline{w^2}\, L^{-2\zeta_{\rm dep}} \sim G(M\, L^{-\zeta_{\rm dep}}). \tag{8}$$

This scaling form is confirmed in Fig. 5(b) and shows that the aspect-ratio parameter $k = ML^{-\zeta_{\rm dep}}$ fully controls the anisotropic finite-size scaling of the problem. It is worth, however, noting some interesting consequences of the result of Fig. 5(b), as we describe below.

Since at very small $k$ the interface is in the random-periodic regime, Eq. (8) should led to $\overline{w^2} \sim L^{2\zeta_{\rm L}}$ and therefore one deduces that,

$$G(k) \sim k^{2(1-\zeta_{\rm L}/\zeta_{\rm dep})}, \quad k \ll k^*, \tag{9}$$

where $k^* = m^* L^{-\zeta_{\rm dep}}$. The fact that the random-periodic roughness exponent $\zeta_{\rm L} = 3/2$ is larger than the random-manifold one $\zeta_{\rm dep} \approx 5/4$ consequently implies an initial decrease of $G(k)$ as $G(k) \sim k^{-2/5}$, as shown in Fig. 5(b) by the solid line. Periodicity effects, or the crossover from random-periodic to random-manifold, thus explain the initial decrease of $G(k)$ seen in Fig. 5(b), or the initial decrease of $\overline{w^2}$ against $M$ for fixed $L$, seen in Fig. 5(a). At this respect, it is then worth noting that the line $\overline{w^2} = M^2$, shown by a dashed line, lies completely in the regime $k < k^*$ implying that the naive criterion $\overline{w^2} < M^2$ is not enough to avoid periodicity effects, and to have the system fully in the random-manifold regime. As we show later, this is related with the shape of the probability distribution of $P(w^2)$ which displays sample-to-sample fluctuations of the order of the average $\overline{w^2}$.

The presence of a minimum at $k^*$ in the function $G(k)$ and in particular its slower than power-law increase for $k > k^*$ is non-trivial and constitutes one of the main results of the present work. This result shows that corrections to the standard scaling $\overline{w^2} \sim L^{\zeta_{\rm dep}}$ may arise from the aspect-ratio dependence of the prefactor $G(k)$. On the one hand, $\overline{w^2}$ now grows with $M$ for $L$ fixed, in spite that $\overline{w^2} \ll M^2$, i.e. transverse-size/periodicity scaling is present. On the other hand, the scaling of $\overline{w^2}$ with

$L$ is slower in this regime, due to subleading scaling corrections coming from $G(k)$. The precise origin of these interesting leading and subleading corrections in the finite-size anisotropic scaling are highly non-trivial. Since the critical configurations in this regime have the constant roughness exponent $\zeta_{\rm dep}$ of the random-manifold universality class, the slow increase of $G(k)$ cannot be attributed to a geometrical crossover effect, as for the case $k < k^*$. However, we might relate this effect to the crossover in the critical force statistics, from Gaussian to Gumbel, in the $k \gg k^*$ limit [32]. In the Gumbel regime, the average critical force is expected to increase as $F_c \sim \log(M/L^{\zeta}_{\rm dep}) \equiv \log k$ [39], since the sample critical force can be roughly regarded as the maximum among $M/L^{\zeta}_{\rm dep}$ independent subcritical forces and configurations [32]. The increase in the critical force might be therefore correlated with the slow increase of roughness. The physical connection between the two is subtle though, since a large critical force in a very elongated sample could be achieved both by profiting very rare correlated pinning forces such as accidental columnar defects, or by profiting very rare non-correlated strong pinning forces. Since in the first case the critical configuration would be more correlated and in general less rough than for less elongated samples (smaller $k$), contrary to our numerical data of Fig. 5(b), we think that the second cause is more plausible. We can thus think that in the $k \gg k^*$ limit of extreme value statistics of $F_c$, the effective disorder strength on the critical configuration increases with $k$. This might be translated into the universal function $G(k)$, such that $\overline{w^2} \approx L^{2\zeta_{\rm dep}} G(k)$ can increase for increasing values of $k$ at fixed $L$ in such regime. A quantitative description of these scaling corrections remains an open challenge.

### ii. Distribution function

We now analyze sample-to-sample fluctuations of the square width $w^2$ by computing its probability distribution $P(w^2)$. This property is relevant as $w^2$ fluctuates even in the thermodynamic limit for critical interfaces with a positive roughness exponent [42]. It has been computed for models with dynamical disorder such as random-walk [43] or Edwards–Wilkinson interfaces [44, 45], the Mullins Herrings model [46] and for non-Markovian Gaussian signals in general [47, 48]. It has also been

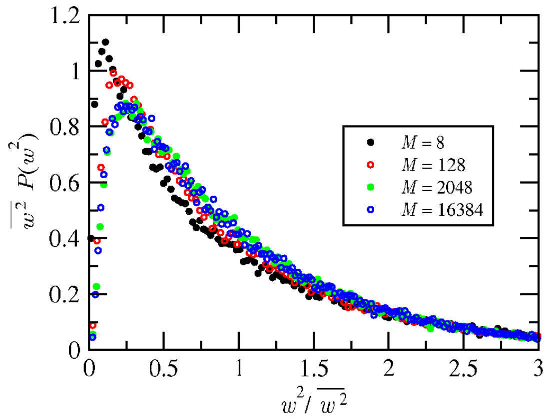


Figure 6: Scaling function $\Phi(x)$ for $L = 256$ and different values of $M = 8, 128, 2048, 16384$, which shows the change with the transverse size $M$.

calculated for non-linear models such as the one-dimensional Kardar–Parisi–Zhang model [49, 50] and for the quenched Edwards–Wilkinson model at equilibrium [51].

In particular, the probability distribution $P(w^2)$ of critical interfaces at the depinning transition was studied analytically [52], numerically [31] and also experimentally for contact lines in partial wetting [7]. Remarkably, non-Gaussian effects in depinning models are found to be smaller than 0.1% [31, 52], thus showing that $P(w^2)$ is strongly determined by the self-affine (critical) geometry itself, rather than by the particular mechanism producing it. As in all the above mentioned systems the width distribution $P(w^2)$ at different universality classes of the depinning transition was found to scale as

$$\overline{w^2} P(w^2) \approx \Phi_\zeta \left( \frac{w^2}{\overline{w^2}} \right). \tag{10}$$

with $\Phi_\zeta$ an universal function, which only depends on the roughness exponent $\zeta$ and on boundary conditions when the global width is considered [47, 48]. In this way, $\overline{w^2}$ is the only characteristic length-scale of the system, absorbing the system longitudinal size $L$, and all the non-universal parameters of the model such as the elastic constant of the interface, the strength of the disorder and/or the temperature. Since $\Phi_\zeta$ can be easily generated using non-Markovian Gaussian signals [53], the quantity $\overline{w^2} P(w^2)$ is a good observable to extract the

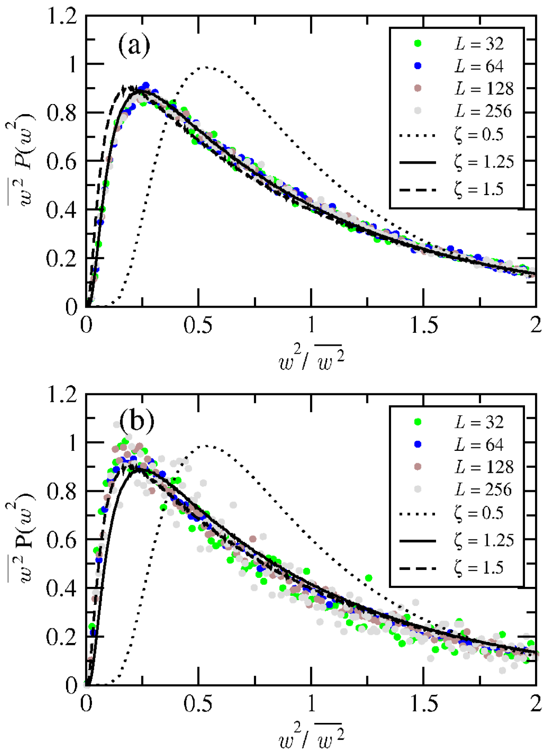


Figure 7: Scaling function $\Phi(x)$ for different values of $L = 32, 64, 128, 256$ while keeping (a) $k = M/L^{\zeta_{\rm dep}} \approx 1$ and (b) $k = M/L^{\zeta_{\rm dep}} \approx 0.025$. The dotted line corresponds to the scaling function of the non-disordered Edwards–Wilkinson equation [43], while the continuous and dashed lines correspond to the scaling functions of Gaussian signals with $\zeta = 1.25$ and $\zeta = 1.5$, respectively [31, 53].

roughness exponent of a critical interface from experimental data.

In Fig. 6, we show how the scaled distribution function $\Phi(x) \equiv \overline{w^2}\, P(x\, \overline{w^2})$ looks like for the depinning transition in a random-periodic medium for a fixed value $L = 256$ and different values of $M$. We see that $\Phi(x)$ depends on $M$ for small $M$ but converges to a fixed shape for large $M$. We also note that for all $M$ $\Phi(x)$ extends appreciably beyond $x = 1$ explaining why the criterion $\overline{w^2} \lesssim M^2$ is not enough to be fully in the random-manifold regime, as noted in Fig. 5.

In Fig. 7, we show the scaling function $\Phi(x)$ for different values of $L$ and $M$ but fixing the aspect-ratio parameter $k = M/L^{\zeta_{\rm dep}}$, $k \approx 1 > k^*$ in Fig. 7(a) and $k \approx 0.025 \ll k^*$ in Fig. 7(b), with $k^*$ the minimum of $\overline{w^2}$. Since data for the same $k$ practically collapses into the same curve, we can write for our case:

$$\overline{w^2} P(w^2) = \Phi\left(\frac{w^2}{\overline{w^2}}, k\right). \tag{11}$$

Therefore, the anisotropic scaling of the probability distribution is fully controlled by $k$, as it was found for $\overline{w^2}$.

In Figs. 7(a) and (b), we also show the universal functions $\Phi_{\zeta_L}$ and $\Phi_{\zeta_{\rm dep}}$ generated using non-Markovian Gaussian signals [31, 53], and for comparison we also show $\Phi_{1/2}$ corresponding to the Markovian periodic Gaussian signal or the Edwards–Wilkinson equation [43]. Comparing this with the collapsed data for depinning, we see that the function $\Phi\left(\frac{w^2}{\overline{w^2}}, k\right)$ respects the limits

$$\begin{aligned} \Phi\left(x, k \to 0\right) &= \Phi_{\zeta_{\rm L}}(x), \\ \Phi\left(x, k \gtrsim k^*\right) &\approx \Phi_{\zeta_{\rm dep}}(x), \end{aligned} \tag{12}$$

as expected from the existence of the geometric crossover between the roughness exponents $\zeta_{\rm L}$ for $k \to 0$ and $\zeta_{\rm dep}$ for $k > k^*$. For intermediate values $k < k^*$, however, $\Phi\left(\frac{w^2}{\overline{w^2}}, k\right)$ does not necessarily coincide with the one of a Gaussian signal function $\Phi_\zeta$ for a given $\zeta$, since the critical configuration includes a crossover length $l^* \lesssim L$. Whether multi-affine or effective exponent self-affine non-Markovian Gaussian signals can be used to describe satisfactorily these intermediate cases is an interesting open issue.

## IV. Conclusions

We have numerically studied the anisotropic finite-size scaling of the roughness of a driven elastic string at its sample-dependent depinning threshold in a random medium with periodic boundary conditions in both the longitudinal and transverse directions. The average square width $\overline{w^2}$ and its probability distribution are both controlled by the parameter $k = M/L^{\zeta_{\rm dep}}$. A non-trivial single minimum for a finite value of $k$ was found in $\overline{w^2}/L^{2\zeta_{\rm dep}}$. For small $k$, the initial decrease of $\overline{w^2}$ reflects the crossover from the random-periodic to the random-manifold roughness. For very large $k$, the growth with $k$ implies that the crossover to Gumbel statistics in the critical forces induces corrections to $G(k)$, that grow with $k$, to the string roughness scaling $\overline{w^2} \approx G(k) L^{2\zeta_{\rm dep}}$. These increasingly rare critical configurations thus have an anomalous roughness scaling: they have a transverse-size/periodicity scaling in spite that its width is $\overline{w^2} \ll M^2$, and subleading (negative) corrections to the standard random-manifold longitudinal-size scaling.

Our results could be useful for understanding roughness fluctuations and scaling in finite experimental systems. The crossover from random-periodic to random-manifold roughness could be studied in periodic elastic systems with variable periodicity, such as confined vortex rows [54] and single-files of macroscopically charged particles [55] or colloids [56], with additional quenched disorder. The rare-event dominated scaling corrections to the interface roughness scaling could be studied in systems with a large transverse dimension, such as domain walls in ferromagnetic nanowires [57]. For the later case, it would be interesting to have a quantitative theory, making the connection between the extreme value statistics of the depinning threshold and the anomalous scaling corrections to the roughness of such rare critical configurations. This would allow to understand the dimensional crossover, from interface to particle depinning.

*Acknowledgements* - This work was supported by CNEA, CONICET under Grant No. PIP11220090100051, and ANPCYT under Grant No. PICT2007886. A. B. K. acknowledges Universidad de Barcelona, Ministerio de Ciencia e Innovación (Spain) and Generalitat de Catalunya for partial funding through I3 program.

[1] S Lemerle, J Ferré, C Chappert, V Mathet, T Giamarchi, P Le Doussal, *Domain wall creep in an Ising ultrathin magnetic film*, Phys. Rev. Lett. **80**, 849 (1998).

[2] M Bauer, A Mougin, J P Jamet, V Repain, J Ferré, S L Stamps, H Bernas, C Chappert, *Deroughening of domain wall pairs by dipolar repulsion*, Phys. Rev. Lett. **94**, 207211 (2005).

[3] M Yamanouchi, D Chiba, F Matsukura, T Dietl, H Ohno, *Velocity of domain-wall motion induced by electrical current in the ferromagnetic semiconductor (Ga,Mn)As*, Phys. Rev. Lett. **96**, 096601 (2006).

[4] P J Metaxas, J P Jamet, A Mougin, M Cormier, J Ferré, V Baltz, B Rodmacq, B Dieny, R L Stamps, *Creep and flow regimes of magnetic domain-wall motion in ultrathin Pt/Co/Pt films with perpendicular anisotropy*, Phys. Rev. Lett. **99**, 217208 (2007).

[5] P Paruch, T Giamarchi, J M Triscone, *Domain wall roughness in epitaxial ferroelectric $PbZr_{0.2}Ti_{0.8}O_3$ thin films*, Phys. Rev. Lett. **94**, 197601 (2005).

[6] P Paruch, J M Triscone, *High-temperature ferroelectric domain stability in epitaxial $PbZr_{0.2}Ti_{0.8}O_3$ thin films*, Appl. Phys. Lett. **88**, 162907 (2006).

[7] S Moulinet, A Rosso, W Krauth, E Rolley, *Width distribution of contact lines on a disordered substrate*, Phys. Rev. E **69**, 035103(R) (2004).

[8] N Martys, M Cieplak, M O Robbins, *Critical phenomena in fluid invasion of porous media*, Phys. Rev. Lett. **66**, 1058 (1991).

[9] I Hecht, H Taitelbaum, *Roughness and growth in a continuous fluid invasion model*, Phys. Rev. E **70**, 046307 (2004).

[10] E Bouchaud, J P Bouchaud, D S Fisher, S Ramanathan, J R Rice, *Can crack front waves explain the roughness of cracks?*, J. Mech. Phys. Solids **50**, 1703 (2002).

[11] M Alava, P K V V Nukalaz, S Zapperi, *Statistical models of fracture*, Adv. Phys. **55**, 349 (2006).

[12] A A Middleton, *Asymptotic uniqueness of the sliding state for charge-density waves*, Phys. Rev. Lett. **68**, 670 (1992).

[13] D S Fisher, *Sliding charge-density waves as a dynamic critical phenomenon*, Phys. Rev. B **31**, 1396 (1985).

[14] O Narayan, D S Fisher, *Critical behavior of sliding charge-density waves in $4-\varepsilon$ dimensions*, Phys. Rev. B **46**, 11520 (1992).

[15] T Nattermann, S Stepanow, L H Tang, H Leschhorn, *Dynamics of interface depinning in a disordered medium*, J. Phys. II **2**, 1483 (1992).

[16] P Le Doussal, K J Wiese, P Chauve, *Two-loop functional renormalization group theory of the depinning transition*, Phys. Rev. B **66**, 174201 (2002).

[17] L B Ioffe, V M Vinokur, *Dynamics of interfaces and dislocations in disordered media*, J. Phys. C: Solid State Phys. **20**, 6149 (1987).

[18] P Chauve, T Giamarchi, P Le Doussal, *Creep and depinning in disordered media*, Phys. Rev. B **62**, 6241 (2000).

[19] A B Kolton, A Rosso, T Giamarchi, *Creep motion of an elastic string in a random potential*, Phys. Rev. Lett. **94**, 047002 (2005).

[20] A B Kolton, A Rosso, T Giamarchi, W Krauth, *Creep dynamics of elastic manifolds via exact transition pathways*, Phys. Rev. B **79**, 184207 (2009).

[21] A B Kolton, A Rosso, T Giamarchi, W Krauth, *Dynamics below the depinning threshold in disordered elastic systems*, Phys. Rev. Lett. **97**, 057001 (2006).

[22] L W Chen, M C Marchetti, *Interface motion in random media at finite temperature*, Phys. Rev. B **51**, 6296 (1995).

[23] D Vandembroucq, R Skoe, S Roux, *Universal depinning force fluctuations of an elastic line: Application to finite temperature behavior*, Phys. Rev. E **70**, 051101 (2004).

[24] U Nowak, K D Usadel, *Influence of temperature on the depinning transition of driven interfaces*, Europhys. Lett. **44**, 634 (1998).

[25] L Roters, A Hucht, S Lübeck, U Nowak, K D Usadel, *Depinning transition and thermal fluctuations in the random-field Ising model*, Phys. Rev. E **60**, 5202 (1999).

[26] S Bustingorry, A B Kolton, T Giamarchi, *Thermal rounding of the depinning transition*, Europhys. Lett. **81**, 26005 (2008).

[27] S Bustingorry, A B Kolton, T Giamarchi, (unpublished).

[28] A Rosso, W Krauth, *Monte Carlo dynamics of driven elastic strings in disordered media*, Phys. Rev. B **65**, 012202 (2001).

[29] A Rosso, W Krauth, *Origin of the roughness exponent in elastic strings at the depinning threshold*, Phys. Rev. Lett. **87**, 187002 (2001).

[30] A Rosso, W Krauth, *Roughness at the depinning threshold for a long-range elastic string*, Phys. Rev. E **65**, 025101(R) (2002).

[31] A Rosso, W Krauth, P Le Doussal, J Vannimenus, K J Wiese, *Universal interface width distributions at the depinning threshold*, Phys. Rev. E **68**, 036128 (2003).

[32] C Bolech, A Rosso, *Universal statistics of the critical depinning force of elastic systems in random media*, Phys. Rev. Lett. **93**, 125701 (2004).

[33] O Duemmer, W Krauth, *Critical exponents of the driven elastic string in a disordered medium*, Phys. Rev. E **71**, 061601 (2005).

[34] A Rosso, P L Doussal, K J Wiese, *Numerical calculation of the functional renormalization group fixed-point functions at the depinning transition*, Phys. Rev. B **75**, 220201 (2007).

[35] A Rosso, P Le Doussal, K J Wiese, *Avalanche-size distribution at the depinning transition: A numerical test of the theory*, Phys. Rev. B **80**, 144204 (2009).

[36] A B Kolton, A Rosso, E V Albano, T Giamarchi, *Short-time relaxation of a driven elastic string in a random medium*, Phys. Rev. B **74**, 140201 (2006).

[37] A B Kolton, G Schehr, P Le Doussal, *Universal nonstationary dynamics at the depinning transition*, Phys. Rev. Lett. **103**, 160602 (2009).

[38] S Bustingorry, A B Kolton, T Giamarchi, *Random-manifold to random-periodic depinning of an elastic interface*, Phys. Rev. B **82**, 094202 (2010).

[39] A A Fedorenko, P Le Doussal, K J Wiese, *Universal distribution of threshold forces at the depinning transition*, Phys. Rev. E **74**, 041110 (2006).

[40] A Rosso, A K Hartmann, W Krauth, *Depinning of elastic manifolds*, Phys. Rev. E **67**, 021602 (2003).

[41] O Narayan, D Fisher, *Threshold critical dynamics of driven interfaces in random media*, Phys. Rev. B **48**, 7030 (1993).

[42] Z Rácz, *Scaling functions for nonequilibrium fluctuations: A picture gallery*, SPIE Proc. **5112**, 248 (2003).

[43] G Foltin, K Oerding, Z Rácz, R L Workman, R K P Zia, *Width distribution for random-walk interfaces*, Phys. Rev. E **50**, R639 (1994).

[44] T Antal, Z Rácz, *Dynamic scaling of the width distribution in Edwards–Wilkinson type models of interface dynamics*, Phys. Rev. E **54**, 2256 (1996).

[45] S Bustingorry, L F Cugliandolo, J L Iguain, *Out-of-equilibrium relaxation of the Edwards–Wilkinson elastic line*, J. Stat. Mech.: Theor. Exp. P09008 (2007).

[46] M Plischke, Z Rácz, R K P Zia, *Width distribution of curvature-driven interfaces: A study of universality*, Phys. Rev. E **50**, 3589 (1994).

[47] A Rosso, R Santachiara, W Krauth, *Geometry of Gaussian signals*, J. Stat. Mech.: Theor. Exp. L08001 (2005).

[48] R Santachiara, A Rosso, W Krauth, *Universal width distributions in non-Markovian Gaussian processes*, J. Stat. Mech.: Theor. Exp. P02009 (2007).

[49] E Marinari, A Pagnani, G Parisi, Z Rácz, *Width distributions and the upper critical dimension of Kardar–Parisi–Zhang interfaces*, Phys. Rev. E **65**, 026136 (2002).

[50] S Bustingorry, *Aging dynamics of non-linear elastic interfaces: The Kardar–Parisi–Zhang equation*, J. Stat. Mech.: Theor. Exp. P10002 (2007).

[51] S Bustingorry, J L Iguain, S Chamon, L F Cugliandolo, D Domínguez, *Dynamic fluctuations of elastic lines in random environments*, Europhys. Lett. **76**, 856 (2006).

[52] P Le Doussal, K J Wiese, *Higher correlations, universal distributions, and finite size scaling in the field theory of depinning*, Phys. Rev. E **68**, 046118 (2003).

[53] W Krauth, *Statistical mechanics: Algorithms and computations*, Oxford University Press, New York (2006).

[54] N Kokubo, R Besseling, P Kes, *Dynamic ordering and frustration of confined vortex rows studied by mode-locking experiments*, Phys. Rev. B **69**, 064504 (2004).

[55] C Coste, J B Delfau, C Even, M S Jean, *Single-file diffusion of macroscopic charged particles*, Phys. Rev. E **81**, 051201 (2010).

[56] S Herrera-Velarde, A Zamudio-Ojeda, R Castañeda-Priego, *Ordering and single-file diffusion in colloidal systems*, J. Chem. Phys. **133**, 114902 (2010).

[57] K J Kim, J C Lee, S M Ahn, K S Lee, C W Lee, Y J Cho, S Seo, K H Shin, S B Choe, H W Lee, *Interdimensional universality of dynamic interfaces*, Nature (London) **458**, 740 (2009).